Biochemical and Biophysical Research Communications 430 (2013) 60–65

Contents lists available at SciVerse ScienceDirect

Biochemical and Biophysical Research Communications

journal homepage: www.elsevier.com/locate/ybbrc

Ca^{2+} influx-dependent refilling of intracellular Ca^{2+} stores determines the frequency of Ca^{2+} oscillations in fertilized mouse eggs

Tooru Takahashi [a], Takashi Kikuchi [b], Yusuke Kidokoro [a], Hideki Shirakawa [b,*]

[a] Department of Applied Physics and Chemistry, The University of Electro-Communications, Tokyo 182-8585, Japan
[b] Department of Engineering Science, The University of Electro-Communications, Tokyo 182-8585, Japan

ARTICLE INFO

Article history:
Received 19 October 2012
Available online 15 November 2012

Keywords:
Mammalian fertilization
Ca^{2+} oscillations
Ca^{2+} influx
Intracellular Ca^{2+} store
Store-operated Ca^{2+} entry

ABSTRACT

On mammalian fertilization, long-lasting Ca^{2+} oscillations are induced in the egg by the fusing spermatozoon. While each transient Ca^{2+} increase in Ca^{2+} concentration ($[Ca^{2+}]$) in the cytosol is due to Ca^{2+} release from the endoplasmic reticulum (ER), Ca^{2+} influx from outside is required for Ca^{2+} oscillations to persist. In this study, we investigated how Ca^{2+} influx is interrelated to the cycle of Ca^{2+} release and uptake by the intracellular Ca^{2+} stores during Ca^{2+} oscillations in fertilized mouse eggs. In addition to monitoring cytosolic $[Ca^{2+}]$ with fura-2, the influx rate was evaluated using Mn^{2+} quenching technique, and the change in $[Ca^{2+}]$ in the ER lumen was visualized with a targeted fluorescent probe. We found that the influx was stimulated after each transient Ca^{2+} release and then diminished gradually to the basal level, and demonstrated that the ER Ca^{2+} stores once depleted by Ca^{2+} release were gradually refilled until the next Ca^{2+} transient to be initiated. Experiments altering extracellular $[Ca^{2+}]$ in the middle of Ca^{2+} oscillations revealed the dependence of both the refilling rate and the oscillation frequency on the rate of Ca^{2+} influx, indicating the crucial role of Ca^{2+} influx in determining the intervals of Ca^{2+} transients. As for the influx pathway supporting Ca^{2+} oscillations to persist, STIM1/Orai1-mediated store-operated Ca^{2+} entry (SOCE) may not significantly contribute, since neither known SOCE blockers nor the expression of protein fragments that interfere the interaction between STIM1 and Orai1 inhibited the oscillation frequency or the influx rate.

1. Introduction

Repetitive increases in cytosolic Ca^{2+} concentration ($[Ca^{2+}]_{cyt}$), or Ca^{2+} oscillations, serve as intracellular signal in response to sustained stimulation by extracellular signaling molecules, and regulate various functions in many types of cells [1]. In mammalian eggs, Ca^{2+} oscillations are induced by the fusion with the spermatozoa and trigger the acrosome reaction and the resumption of meiosis [2]. Ca^{2+} oscillations are essentially due to repetitive Ca^{2+} releases from the endoplasmic reticulum (ER) induced by inositol 1,4,5-trisphosphate (IP_3) [3]. A sperm-specific isozyme of phospholipase C, PLCζ, is proposed to be a Ca^{2+} oscillation-inducing factor that diffuses from the sperm into the egg cytoplasm and produces IP_3 by hydrolyzing phosphatidylinositol 4,5-bisphosphate [4]. The cytosolic concentration of IP_3 ($[IP_3]_{cyt}$) increases and is kept elevated [5], and the cycle of Ca^{2+} release through IP_3 receptor/Ca^{2+} channel [6] and Ca^{2+} uptake into the ER repeats to generate periodic changes in $[Ca^{2+}]_{cyt}$ for hours.

The influx of Ca^{2+} from outside the egg is necessary for maintaining Ca^{2+} oscillations, as suggested by the fact that the chelation or removal of extracellular Ca^{2+} results in the reduction in frequency or the abrupt cessation of the oscillations [7,8]. Studies using Mn^{2+} quenching technique have shown that the rate of cation influx was enhanced during Ca^{2+} oscillations induced either by insemination [9] or by the injection of sperm extract [10]. As for the pathway of Ca^{2+} influx, the store-operated Ca^{2+} (SOC) entry (SOCE), which is activated by the depletion of intracellular Ca^{2+} stores [11], has been suggested by the result that the Ca^{2+} influx was accelerated in the eggs treated with thapsigargin, an inhibitor for Ca^{2+} pump on the ER membrane [8,9]. Furthermore, STIM1 and Orai1, an ER membrane protein that works as the sensor for Ca^{2+} concentration in the ER lumen ($[Ca^{2+}]_{ER}$) [12] and a plasma membrane protein that forms SOC channel [13], respectively, have recently been shown to be expressed in mouse eggs and change their distribution to colocalize in response to the depletion of Ca^{2+} stores [14,15], implying that these proteins would mediate SOCE in mouse eggs. It is still uncertain, however, that SOCE plays significant role in the maintenance of Ca^{2+} oscillations at fertilization.

To further elucidate the mechanism for the activation of Ca^{2+} influx and its role in sperm-induced Ca^{2+} oscillations, the

* Corresponding author. Address: Department of Engineering Science, The University of Electro-Communications, 1-5-1 Chofugaoka, Chofu, Tokyo 182-8585, Japan. Fax: +81 42 443 5501.
E-mail address: hshrkw@pc.uec.ac.jp (H. Shirakawa).

0006-291X/$ - see front matter © 2012 Elsevier Inc. All rights reserved.
http://dx.doi.org/10.1016/j.bbrc.2012.11.024

information about the changes in the rate of Ca^{2+} influx and $[Ca^{2+}]_{ER}$ is important. In the present study, we investigated the time course of the activation of cation influx in relation to transient Ca^{2+} releases. Changes in $[Ca^{2+}]_{ER}$ during Ca^{2+} oscillations were analyzed based on the measurements with a genetically encoded ER-targeted fluorescent Ca^{2+} probe. We carried out experiments to address the role of Ca^{2+} influx in Ca^{2+} oscillations, by revealing the impact of the influx rate not only on Ca^{2+} oscillations, but also on the process of refilling the ER Ca^{2+} stores.

2. Materials and methods

2.1. Preparation of cDNA and RNA

The cDNA of cameleon D1ER [16], an ER-targeted Ca^{2+} probe based on fluorescence resonance energy transfer (FRET) between two different GFP variants, was kindly donated by Dr. R.Y. Tsien. The cDNAs of Orai1 and STIM1 were cloned by RT-PCR from brain mRNA of B6 mouse, using SuperScript III reverse transcriptase (Invitrogen, Carlsbad, CA). The N-terminal cytoplasmic domain of Orai1 (amino acid residues 1–90; Orai1-NT) and the C-terminal cytoplasmic domain of STIM1 (amino acid residues 238–685; STIM1-CT) were amplified by PCR with PrimeStar DNA polymerase (Takara Bio, Shiga, Japan) using primers of following sequences: 5′-AACTCGAGATGCATCCGGAGCCTGCC-3′ (Orai1-NT forward), 5′-TTGCGGCCGCCTTAAGCTTTGAGCTTGGCGC-3′ (Orai1-NT reverse), 5′-AACTCGAGAAGGAGCACATGAAGAAAATG-3′ (STIM1-CT forward), and 5′-TTGCGGCCGCCTACTTCTTAAGAGGCTTCTTAA-3′ (STIM1-CT reverse). Short fragment of STIM1 corresponding to the coiled-coil region in the cytoplasmic domain (amino acid residues 339–444; STIM1-CCb9) [17] was amplified using primers with the sequences of 5′-AACTCGAGAGCTCATGGTATGCTCCTG-3′ and 5′-TTGCGGCCGCCTAGTTATTGACAATCTGGAAACCG-3′. The PCR products were inserted at 3′-end of Venus cDNA (a variant of yellow fluorescent protein). For *in vitro* transcription, cDNAs were subcloned into pGLS/$(A)_{21}$x8 vector, which has been constructed by replacing poly$(A)_{30}$ tail in the 3′-untranslated region of pTNT vector (Promega, Madison, WI) with eight tandem repeats of 21-residue oligo(A) intervened by 6-residue spacers. Using these constructs as templates, RNAs were synthesized and purified as described previously [5].

2.2. Preparation of gametes

Procedures to collect mature eggs at metaphase II or immature oocytes at germinal vesicle stage from female mice, and those to collect spermatozoa from male mice and to capacitate them for *in vitro* fertilization, were as described previously [5,18], except the strain of mice (ddY). In some experiments, mature eggs were injected with either Orai1-NT, STIM1-CT, or STIM1-CCb9 RNA diluted in 150 mM KCl, and incubated for 3 h at 37 °C before insemination.

2.3. Ca^{2+} imaging

Eggs were loaded with 2 μM fura-2 AM (Dojindo, Kumamoto, Japan) in M2 medium [18] for 10 min at 37 °C, treated with acidic Tyrode's solution (pH 2.5) to remove zona pellucida, and placed in M2 medium heated at 32–34 °C on the stage of fluorescence microscope (Axiovert S-100, Carl Zeiss, Oberkochen, Germany). A small volume of medium containing capacitated sperm was added for insemination. A series of fluorescence images through a filter of 535 ± 12 nm was captured with ICCD camera (ICCD-350F, VideoScope, Toronto, Canada) at constant intervals, alternating excitation wavelengths by switching filters of 340 ± 5 nm and 380 ± 5 nm. Fluorescence ratio of 340 nm to 380 nm (F_{340}/F_{380}) was taken as the index of $[Ca^{2+}]_{cyt}$. In some experiments, M2 medium containing SOCE blocker, such as SKF-96365 (Sigma–Aldrich, St. Luis, MO) and 2-aminoethoxydiphenylborane (2-APB) (Sigma–Aldrich), was added after insemination, to examine their effects on Ca^{2+} oscillations.

2.4. Mn^{2+} quenching

Time-lapse fluorescence images of fura-2-loaded eggs were recorded in the same way as Ca^{2+} imaging described above, except a filter of 360 nm instead of 380 nm was used for excitation. M2 medium containing $MnCl_2$ was added 60–80 min after the onset of Ca^{2+} oscillations, giving a final concentration of 0.5 mM. A series of fluorescence intensities at 360-nm excitation (F_{360}) was normalized by the value before Mn^{2+} addition (F_0). The slope of F_{360}/F_0 (in percentage) for the last 5 min before Mn^{2+} addition was subtracted from that for the first 2.5 min after the addition, to obtain the value

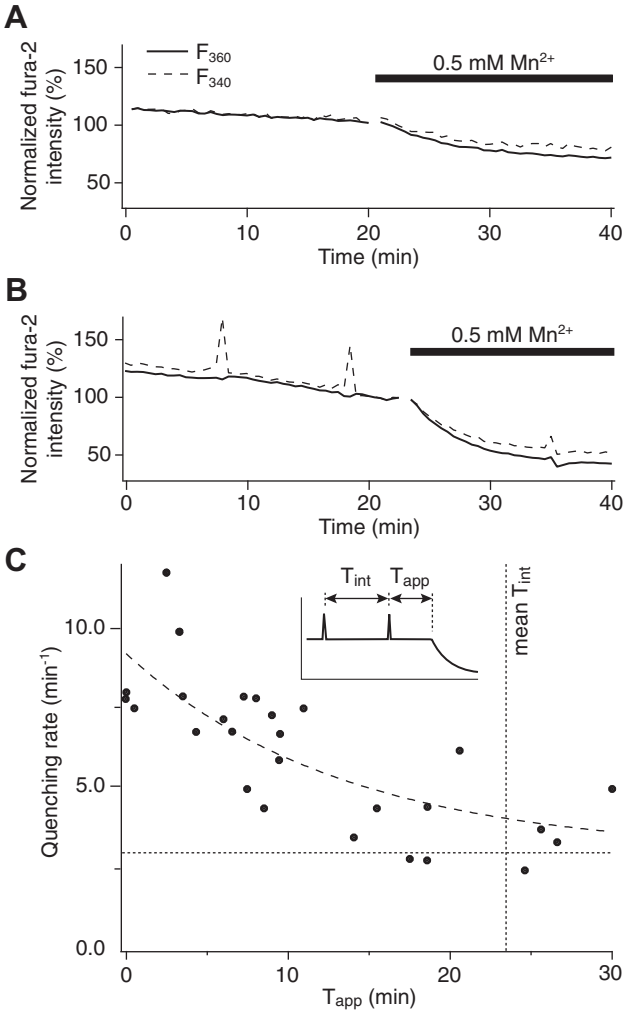

Fig. 1. The quenching of fura-2 fluorescence due to Mn^{2+} entry during sperm-induced Ca^{2+} oscillations. Typical changes in fluorescence intensities of fura-2 excited at 360 nm (solid trace) and 340 nm (dashed trace) are shown for an unfertilized egg (A) and a fertilized egg (B). Mn^{2+} (0.5 mM) was added to the extracellular medium as indicated by the horizontal bar. In (C), initial rates of Mn^{2+} quenching in fertilized eggs are plotted against the time from the last preceding Ca^{2+} transient to Mn^{2+} application (T_{app}). The mean rate of Mn^{2+} quenching in unfertilized eggs is indicated by the horizontal dotted line. The vertical dotted line indicates the average of the interval between the last two Ca^{2+} transients preceding Mn^{2+} application (T_{int}) for all the eggs analyzed for the plot (23.4 ± 7.8 min, mean ± SD, n = 27).

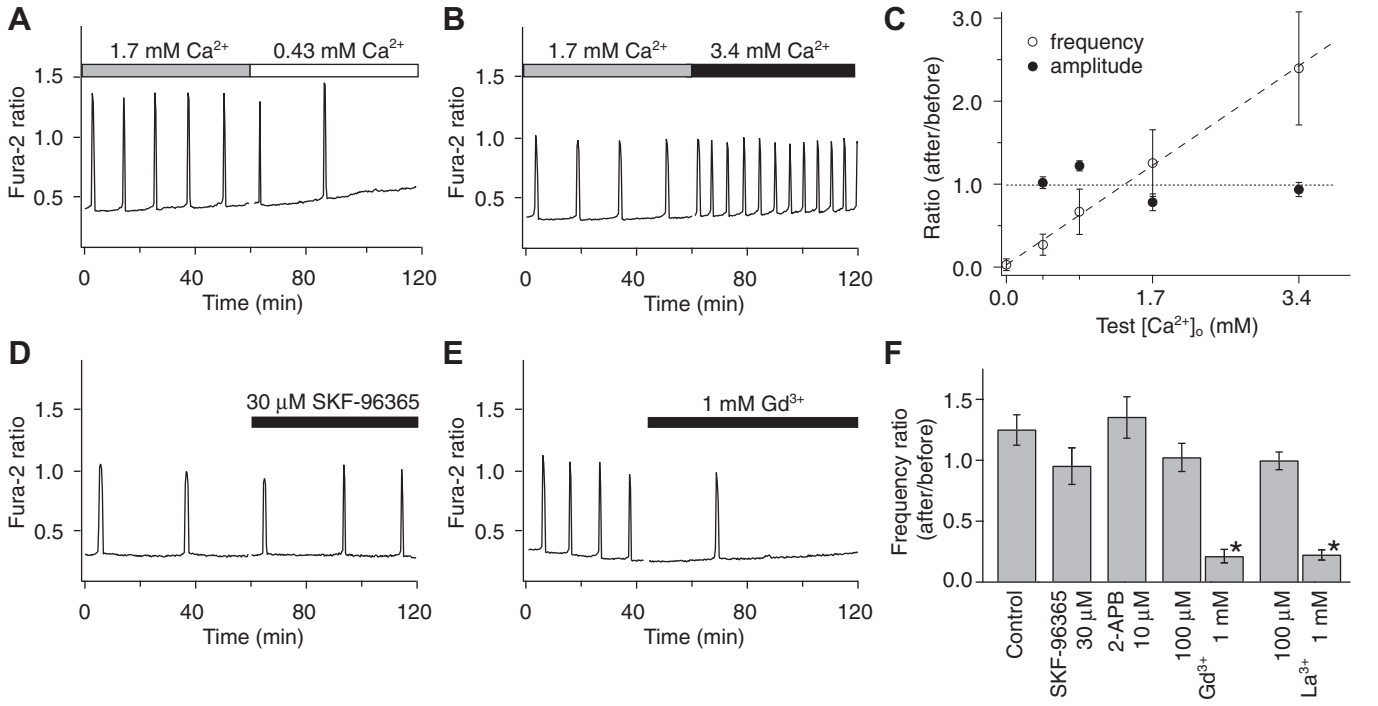

Fig. 2. The effects of $[Ca^{2+}]_o$ and SOCE inhibitors on sperm-induced Ca^{2+} oscillations. In the middle of Ca^{2+} oscillations, $[Ca^{2+}]_o$ was changed from the default concentration in M2 medium (1.7 mM) to the test concentration of 0.43 mM (A) or 3.4 mM (B), while changes in $[Ca^{2+}]_{cyt}$ were monitored by fura-2 ratio (F_{340}/F_{360}). The numbers and mean amplitudes of Ca^{2+} transients during 90 min before and after the alteration of $[Ca^{2+}]_o$ were measured, and their ratios (after/before) were plotted against the test $[Ca^{2+}]_o$ in (C), as mean values ± SD for at least five eggs. In (D) and (E), 30 μM SKF-96365 or 1 mM $GdCl_3$ was added to the extracellular medium, respectively. Frequency ratios before and after the applications of SOCE blockers (SKF-96365, 2-APB, Gd^{3+} and La^{3+}) are summarized in (F), as mean values ± SEM for at least six eggs. The asterisk indicates significant difference compared with mock control (one-way ANOVA, $p < 0.01$).

representing the initial rate of Mn^{2+} quenching corrected for the bleaching rate of fura-2 fluorescence.

2.5. Measurement of $[Ca^{2+}]_{ER}$

The methods of introducing D1ER into the eggs and of recording D1ER fluorescence signals were essentially the same as those described for FRET-based IP_3 probes [5]. Immature oocytes were injected with D1ER RNA and were maturated *in vitro* for 16 h. After loaded with fura-2, eggs were illuminated with 450-nm light to excite ECFP in D1ER, and fluorescence signals emitted from ECFP and citrine were detected at 480 ± 15 nm and 535 ± 12 nm, respectively. Fura-2 fluorescence was detected at 535 nm with excitation wavelengths of 340 nm and 380 nm. The ratio of citrine to ECFP fluorescence (Y/C ratio), which increases by the structural change of D1ER due to Ca^{2+} binding [16], was calculated as the index for $[Ca^{2+}]_{ER}$, whereas $[Ca^{2+}]_{cyt}$ was represented by fura-2 ratio (F_{340}/F_{380}). To examine the intracellular localization of expressed D1ER, some eggs were observed with a confocal microscope (CSU10, Yokogawa Electric, Tokyo, Japan), using 488-nm line of Ar–Kr laser for excitation and 525 ± 15 nm barrier filter for emission.

3. Results and discussion

3.1. Divalent cation influx during sperm-induced Ca^{2+} oscillations

Adding Mn^{2+} to extracellular medium enables us to evaluate Ca^{2+} influx, although indirectly, as a decrease in fluorescence intensity of a fura-2-loaded cell, because Mn^{2+} that enters through Ca^{2+} influx channel binds to fura-2 in the cytosol and quenches its fluorescence. By this method, McGuinness et al. [9] have demonstrated the enhancement of cation influx linked to Ca^{2+} transients in early phase of Ca^{2+} oscillations in fertilized mouse eggs. However, the time course of the changes in the influx rate during intervals between Ca^{2+} transients remains unresolved.

Mn^{2+} was added to unfertilized eggs, or to fertilized eggs in the middle of steady Ca^{2+} oscillations (Fig. 1A and B). The initial quenching rate of fura-2 was, on average, ~2-fold larger in fertilized eggs (6.1 ± 2.3 min^{-1}; mean ± SD, $n = 27$) than in unfertilized eggs (3.3 ± 0.6 min^{-1}, $n = 12$). The cation influx during Ca^{2+} oscillations was further analyzed in relation to the timing of Ca^{2+} transients, by collectively plotting the quenching rates in fertilized eggs against the time of Mn^{2+} application after the last preceding Ca^{2+} transient (Fig. 1C). It is clear that the quenching rate was larger in the eggs exposed to Mn^{2+} immediately after Ca^{2+} transient, and was smaller when exposed after longer interval. The maximal rate and the decay time constant, obtained by exponential curve fitting for triplicate experiments, were 10.6 ± 2.5 min^{-1} and 11.2 ± 0.8 min (mean ± SD), respectively. Thus it was demonstrated that the cation influx is stimulated approximately 3-fold after each Ca^{2+} transient and gradually subsides toward the basal level until the next transient occurs.

3.2. Effects of Ca^{2+} influx on Ca^{2+} oscillations

When Ca^{2+} influx was decelerated by decreasing extracellular Ca^{2+} concentration ($[Ca^{2+}]_o$) amid persisting Ca^{2+} oscillations, the frequency of Ca^{2+} transients was decreased (Fig. 2A). The frequency was increased when Ca^{2+} influx was accelerated by raising $[Ca^{2+}]_o$ (Fig. 2B). The ratio of the oscillation frequencies before and after the alteration of $[Ca^{2+}]_o$ was linearly dependent on the test $[Ca^{2+}]_o$ and, therefore, on the rate of Ca^{2+} influx (Fig. 2C). The amplitude of Ca^{2+} transient was not significantly affected by the alteration of the influx rate. Among some known SOCE inhibitors [11], 30 μM SKF-96365 and 10 μM 2-APB had no effect on Ca^{2+} oscillations (Fig. 2D and F). Both Gd^{3+} and La^{3+} inhibited the oscil-

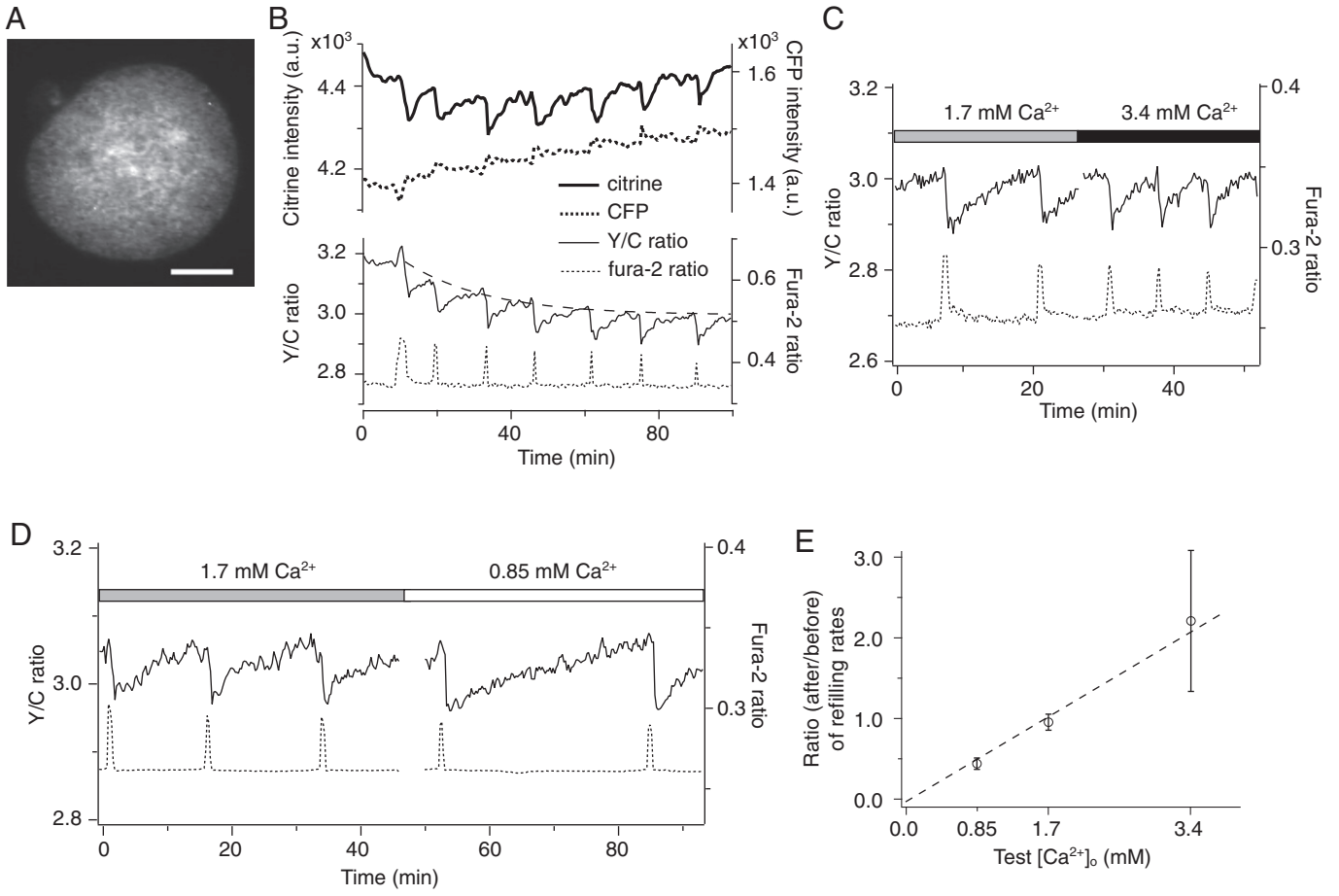

Fig. 3. Changes in $[Ca^{2+}]_{ER}$ during sperm-induced Ca^{2+} oscillations and their dependence on $[Ca^{2+}]_o$. The confocal fluorescence image in (A) represents typical intracellular localization of D1ER expressed in the egg maturated *in vitro*. The bar corresponds to 20 μm. Oscillatory changes in $[Ca^{2+}]_{ER}$ and $[Ca^{2+}]_{cyt}$ in a fertilized egg are demonstrated in (B), as D1ER ratio (Y/C ratio; thin solid trace) and fura-2 ratio (F_{340}/F_{380}; thin dotted trace), respectively. Fluorescence intensities of citrine (thick solid trace) and CFP (thick dotted trace) changed in the opposite directions at each Ca^{2+} transient, as expected for the fluorescence signal from the FRET-based probe. Dashed curve indicates the threshold $[Ca^{2+}]_{ER}$ level at which Ca^{2+} transients occurred. Typical changes in the time course of $[Ca^{2+}]_{ER}$ by the alteration of $[Ca^{2+}]_o$ are shown in (C) and (D). Time constant of Ca^{2+} refilling (τ) was calculated by fitting single exponential curve to the values of Y/C ratio during rising phase following each Ca^{2+} release. The refilling rates ($1/\tau$) were averaged for Ca^{2+} transients observed in 60 min before and after the alteration of $[Ca^{2+}]_o$, and their ratio (after/before) was plotted against the test $[Ca^{2+}]_o$ in (E) (mean ± SD, for at least five eggs).

lations, but millimolar concentrations were required (Fig. 2E and F). The insensitiveness to SOCE inhibitors has recently been reported for Ca^{2+} oscillations induced by intracytoplasmic sperm injection (ICSI) [19]. Thus it is suggested that, although SOCE may be activated at fertilization in some extent, it does not have a significant role in maintaining Ca^{2+} oscillations in mouse eggs.

3.3. Refilling of Ca^{2+} stores after Ca^{2+} release

Fluorescence in the egg that had been injected with D1ER RNA and maturated *in vitro*, showed meshwork pattern of localization characteristic to intracellular distribution of the ER [20] (Fig. 3A). When the eggs expressing D1ER were fertilized, the changes in $[Ca^{2+}]_{ER}$ during Ca^{2+} oscillations were clearly observed as those in Y/C ratio of D1ER fluorescence. As shown in Fig. 3B, $[Ca^{2+}]_{ER}$ rapidly decreased at each Ca^{2+} transient and then increased gradually until the next transient occurred, indicating the cycle of Ca^{2+} release and uptake by the ER Ca^{2+} stores. The time constant of refilling by Ca^{2+} uptake, calculated by exponential curve fitting to data obtained in eight eggs, was 7.1 ± 3.3 min (mean ± SD). The time course of refilling was much slower compared to the rapid decrease in $[Ca^{2+}]_{cyt}$ after Ca^{2+} release. Taken together with the previous study of numerical simulation [10] suggesting that Ca^{2+} extrusion to outside the egg is much slower than Ca^{2+} uptake, most of released Ca^{2+} would bind quickly to abundant Ca^{2+}-binding proteins in the cytoplasm.

Refilling of the ER after Ca^{2+} transient was accelerated by doubling $[Ca^{2+}]_o$ (Fig. 3C), and was decelerated by reducing $[Ca^{2+}]_o$ by half amid Ca^{2+} oscillations (Fig. 3D). Quantitative analysis showed that the refilling rate was, like the oscillation frequency, linearly dependent on $[Ca^{2+}]_o$ and therefore on Ca^{2+} influx rate (Fig. 3E). This result indicates that Ca^{2+} influx determines the interval between Ca^{2+} transients by affecting the refilling rate of the ER Ca^{2+} stores; Ca^{2+} content in the stores must be restored to a certain threshold level for the next Ca^{2+} transient to be initiated by regenerative Ca^{2+} release through IP_3R/Ca^{2+} channel. According to this model, Ca^{2+} transient can be initiated at lower $[Ca^{2+}]_{ER}$ level when $[IP_3]_{cyt}$ is higher. The fact that $[Ca^{2+}]_{ER}$ at which each Ca^{2+} transient was initiated became lower after the onset of Ca^{2+} oscillations (see dashed curve in Fig. 3B), is consistent with the elevation of $[IP_3]_{cyt}$ observed in the early phase of fertilization [5].

3.4. Role of STIM/Orai-mediated SOCE in Ca^{2+} oscillations

Neither frequencies nor amplitudes of sperm-induced Ca^{2+} oscillations were affected by the expression of Orai1-NT or

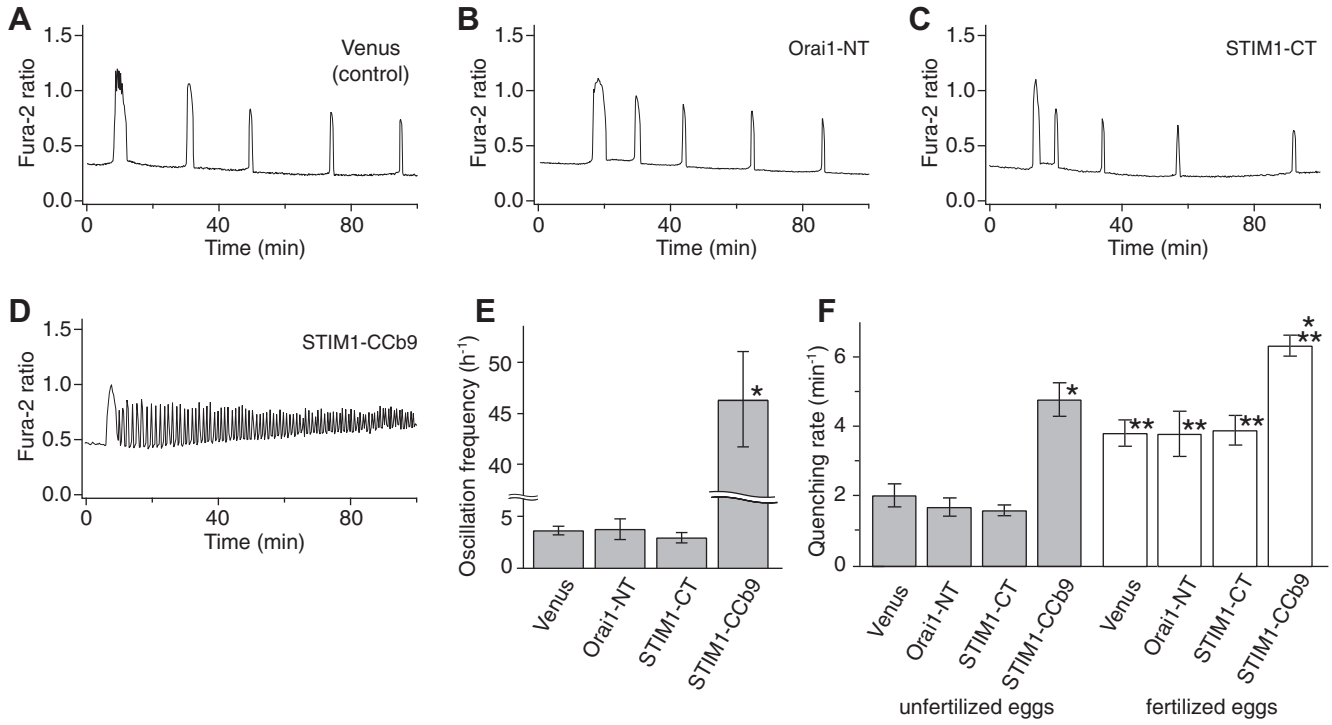

Fig. 4. Effects of cytoplasmic domain fragments of STIM1 and Orai1 on sperm-induced Ca^{2+} oscillations and the cation influx rate. Typical examples of sperm-induced Ca^{2+} oscillations in the eggs expressing Venus (control), Orai1-NT, STIM1-CT, or STIM1-CCb9 are shown as the changes in fura-2 ratio in (A)–(D). Frequencies of Ca^{2+} oscillations, calculated from the number of Ca^{2+} transients observed during 120 min after the first Ca^{2+} increase (not including itself), and the initial quenching rates of fura-2 fluorescence in unfertilized and fertilized eggs upon the application of 0.5 mM Mn^{2+} are summarized in (E) and (F), respectively, as mean ± SEM for at least eight eggs. Single and double asterisks indicate significant difference compared with Venus-expressing control eggs and with unfertilized eggs, respectively ($p < 0.01$).

STIM1-CT (Fig. 4A–C), both of which interfere the interaction between intrinsic Orai1 and STIM1 proteins [17,21]. In contrast, the expression of STIM1-CCb9 remarkably accelerated the oscillations (Fig. 4D and E). STIM1-CCb9, which can activate Ca^{2+} influx through Orai1 channels [17], enhanced the rate of Mn^{2+} entry in both unfertilized and fertilized eggs (Fig. 4F), suggesting that Orai1-mediated Ca^{2+} entry in the egg can be stimulated by STIM1 and, if activated, can contribute by supplying Ca^{2+} to refill the ER stores. It should be noted, however, that the augmenting effect of STIM1-CCb9 on the oscillation frequency (~10-fold, Fig. 4E) was much larger than expected from that on the influx rate in fertilized eggs (~1.5-fold, Fig. 4F). STIM1 may have alternative role in Ca^{2+} mobilization during Ca^{2+} oscillations, regulating, for example, the uptake of Ca^{2+} into the ER by Ca^{2+} pump or the release through IP_3R/Ca^{2+} channels.

Apparent similarity of the temporal changes in cation influx rate and in $[Ca^{2+}]_{ER}$ during the interval of Ca^{2+} transients (see Figs. 1C and 3B) might suggest SOCE as the pathway activated after Ca^{2+} release. However, the result that both STIM1-CT and Orai1-NT failed to affect sperm-induced Ca^{2+} oscillations or the rate of cation influx (Fig. 4E and F), together with the ineffectiveness of known SOCE inhibitors in suppressing Ca^{2+} oscillations, suggests that STIM1/Orai1 pathway is not the dominant route of Ca^{2+} entry for supplying Ca^{2+} to replenish the deleted Ca^{2+} stores. Recently, it was reported that Ca^{2+} oscillations were disrupted in fertilized porcine eggs in which either intrinsic STIM1 or Orai1 was downregulated by RNAi [22,23]. Since even the first Ca^{2+} increase was abnormally small in either STIM1- or Orai1-knockdown eggs, STIM1/Orai1-mediated Ca^{2+} entry may be required in the process of maturation to establish Ca^{2+} mobilizing machinery by the time of fertilization.

In summary, the present study revealed the intimate interrelationship between Ca^{2+} release, uptake and influx to generate long-lasting Ca^{2+} oscillations in fertilized mouse eggs. Ca^{2+} influx is activated after transient Ca^{2+} release, and Ca^{2+} uptake is facilitated by Ca^{2+} influx, replenishing the Ca^{2+} stores enough for the next Ca^{2+} release to be initiated. Further studies are required to identify the pathway of Ca^{2+} release-activated Ca^{2+} influx, other than STIM1/Orai1-mediated SOCE, responsible for the Ca^{2+} oscillations.

Acknowledgments

We thank Dr. R.Y. Tsien for donating D1ER cDNA. This work was supported by Grand-in-Aid for Scientific Research (C) to H.S. from the Ministry of Education, Culture, Sports, Science and Technology, Japan.

References

[1] M.J. Berridge, G. Dupont, Spatial and temporal signaling by calcium, Curr. Opin. Cell Biol. 6 (1994) 267–274.

[2] D. Kline, J.T. Kline, Repetitive calcium transients and the role of calcium in exocytosis and cell activation in the mouse egg, Dev. Biol. 149 (1992) 80–89.

[3] S. Miyazaki, H. Shirakawa, K. Nakada, Y. Honda, Essential role of the inositol 1,4,5-trisphosphate receptor/Ca^{2+} channel in Ca^{2+} waves and Ca^{2+} oscillations at fertilization of mammalian eggs, Dev. Biol. 158 (1993) 62–78.

[4] C.M. Saunders, M.G. Larman, J. Parrington, L.J. Cox, J. Royse, L.M. Blayney, K. Swann, F.A. Lai, PLCζ: a sperm-specific trigger of Ca^{2+} oscillations in eggs and embryo development, Development 129 (2002) 3533–3544.

[5] H. Shirakawa, M. Ito, M. Sato, Y. Umezawa, S. Miyazaki, Measurement of intracellular IP_3 during Ca^{2+} oscillations in mouse eggs with GFP-based FRET probe, Biochem. Biophys. Res. Commun. 345 (2006) 781–788.

[6] S. Miyazaki, M. Yuzaki, K. Nakada, H. Shirakawa, S. Nakanishi, S. Nakade, K. Mikoshiba, Block of Ca^{2+} wave and Ca^{2+} oscillation by antibody to the inositol 1,4,5-trisphosphate receptor in fertilized hamster eggs, Science 257 (1991) 251–255.

[7] Y. Igusa, S. Miyazaki, Effects of altered extracellular and intracellular calcium concentration on hyperpolarizing responses of the hamster egg, J. Physiol. 340 (1983) 611–632.

[8] D. Kline, J.T. Kline, Thapsigargin activates a calcium influx pathway in the unfertilized mouse egg and suppresses repetitive calcium transients in the fertilized egg, J. Biol. Chem. 267 (1992) 17624–17630.

[9] O.M. McGuinness, R.B. Moreton, M.H. Johnson, M.J. Berridge, A direct measurement of increased divalent cation influx in fertilized mouse oocytes, Development 122 (1996) 2199–2206.

[10] T. Mohri, H. Shirakawa, S. Oda, M.S. Sato, K. Mikoshiba, S. Miyazaki, Analysis of Mn^{2+}/Ca^{2+} influx and release during Ca^{2+} oscillations in mouse eggs injected with sperm extract, Cell Calcium 29 (2001) 311–325.

[11] A.B. Parekh, J.W. Putney Jr., Store-operated calcium channels, Physiol. Rev. 85 (2005) 757–810.

[12] J. Liou, M.L. Kim, W.D. Heo, J.T. Jones, J.W. Myers, J.E. Ferrell Jr., T. Meyer, STIM is a Ca^{2+} sensor essential for Ca^{2+}-store-depletion-triggered Ca^{2+} influx, Curr. Biol. 15 (2005) 1235–1241.

[13] M. Prakriya, S. Feske, Y. Gwack, S. Srikanth, A. Rao, P.G. Hogan, Orai1 is an essential pore subunit of the CRAC channel, Nature 443 (2006) 230–233.

[14] C. Gomes-Fernandez, E. Pozo-Guisado, M. Ganan-Parra, M.J. Perianes, I.S. Alvarez, F.J. Martin-Romero, Relocalization of STIM1 in mouse oocytes at fertilization: early involvement of store-operated calcium entry, Reproduction 138 (2009) 211–221.

[15] C. Gomez-Fernandez, A.M. Lopez-Guerrero, E. Pozo-Guisado, I.S. Alvarez, F.J. Martin-Romero, Calcium signaling in mouse oocyte maturation: the roles of STIM1, ORAI1 and SOCE, Mol. Hum. Reprod. 18 (2012) 194–203.

[16] A.E. Palmer, C. Jin, J.C. Reed, R.Y. Tsien, Bcl-2-mediated alteration in endoplasmic reticulum Ca^{2+} analyzed with an improved genetically encoded fluorescent sensor, Proc. Natl. Acad. Sci. U.S.A. 101 (2004) 17404–17409.

[17] T. Kawasaki, I. Lange, S. Feske, A minimal regulatory domain in the C terminus of STIM1 binds to and activates ORAI1 CRAC channels, Biochem. Biophys. Res. Commun. 385 (2009) 49–54.

[18] J. Kumakiri, S. Oda, K. Kinoshita, S. Miyazaki, Involvement of Rho family G proteins in the cell signaling for sperm incorporation during fertilization of mouse eggs: inhibition by *Clostridium difficile* toxin B, Dev. Biol. 260 (2003) 522–535.

[19] Y.-L. Miao, P. Stein, W.N. Jefferson, E. Padilla-Banks, C.J. Williams, Calcium influx-mediated signaling is required for complete mouse egg activation, Proc. Natl. Acad. Sci. U.S.A. 109 (2012) 4169–4174.

[20] G. FitsHarris, P. Marangos, J. Carroll, Cell cycle-dependent regulation of structure of endoplasmic reticulum and inositol 1,4,5-trisphosphate-induced Ca^{2+} release in mouse oocytes and embryos, Mol. Biol. Cell 14 (2003) 288–301.

[21] Y. Takahashi, M. Murakami, H. Watanabe, H. Hasegawa, T. Ohba, Y. Murahisa, K. Nobori, K. Ono, T. Iijima, H. Ito, Essential role of the N-terminus of murine Orai1 in store-operated Ca^{2+} entry, Biochem. Biophys. Res. Commun. 356 (2007) 45–52.

[22] K. Lee, C. Wang, Z. Machaty, STIM1 is required for Ca^{2+} signaling during mammalian fertilization, Dev. Biol. 367 (2012) 154–162.

[23] C. Wang, K. Lee, E. Gajdosci, A.B. Papp, Z. Machaty, Orai1 mediates store-operated Ca^{2+} entry during fertilization in mammalian oocytes, Dev. Biol. 365 (2012) 414–423.